MDPI

Article

Sensitivity of the Viscous Damping Coefficient of Carbon Fiber in Carbon-Fiber-Reinforced Plastic with Respect to the Fiber Angle

Chan-Jung Kim

Department of Mechanical Design Engineering, Pukyong National University, Busan 48513, Korea;
cjkim@pknu.ac.kr; Tel.: +82-51-629-6169

Abstract: The variation in the viscous damping coefficient with the carbon fiber angle can be evaluated using the partial derivatives of the viscous damping coefficient with respect to the resonance frequency and modal damping ratio. However, the direct derivatives of the viscous damping coefficient were not effective solutions to the sensitivity analysis of carbon-fiber-reinforced plastic (CFRP) structures because the viscous damping from the binding matrix was not changed over the carbon fiber angle. If the identified viscous damping coefficients were assumed to be equivalent values from the parallel relationship between the binding matrix and carbon fiber, the relative error of the viscous damping coefficient of carbon fiber between the increased carbon fiber angle and reference angle could be used as the sensitivity index for the viscous damping coefficient of carbon fiber only. The modal parameters, resonance frequency, and modal damping ratio were identified from the experimental modal test of rectangular CFRP specimens for five different carbon fiber angles between 0° and 90°. The sensitivity of the viscous damping coefficient of carbon fiber was determined for two sensitivity indices: the direct derivative of the mass-normalized equivalent viscous damping coefficient and the relative error of the viscous damping coefficient of carbon fiber. The sensitivity results were discussed using the five mode shapes of the CFRP specimen, that is, three bending modes and two twisting modes.

Keywords: viscous damping coefficient; sensitivity analysis; experimental modal analysis; carbon fiber angle; carbon fiber reinforced plastic

1. Introduction

The demand for lightweight materials is increasing, owing to the requirement of energy saving or high efficiency in the operation of mechanical systems; therefore, magnesium, titanium, or other composite materials have been utilized in many industries instead of conventional steel materials. Carbon-fiber-reinforced plastic (CFRP) is a well-known lightweight material that has been used in moving transformation systems, i.e., automobiles, bicycles, and ships, owing to the superior strength-to-weight ratio of CFRP. Mass production of CFRP can help to achieve a reasonable production cost, and many reference data regarding engineering issues have been reported [1–6]. The anisotropic nature of CFRP is unique and beneficial for enhancing structural stiffness in a load-bearing system. However, a sound understanding of the mechanical properties of carbon fiber under different conditions is necessary for the efficient usage of CFRP in field applications [7–9].

Modal analysis is a popular method for identifying the modal parameters to be used in the analysis of dynamic behavior under high spectral loading cases. Several modal parameters, such as resonance frequency, modal damping coefficient, and mode shape vector, can be obtained by measuring the force data and response data [10,11]. The force signal can be achieved from an exciter or impact hammer, and the response data are usually measured by an accelerometer. The dynamics of CFRP structures were also identified via modal testing under the assumption of a linear system [12–14]. The measured modal

damping coefficients showed a relatively large value compared with other lightweight materials [15,16]. The major reason for the high damping coefficient is attributed to the binding matrix because most of the binding matrix in CFRP is used by high-damping materials, such as resin, epoxy, etc.

The damping coefficient identification of CFRP has been reported in several studies [17–19] under the resonance behavior of CFRP structures. The elastic modulus and material damping coefficient were measured using a material testing equipment [17,18]. In a recent study, the variation of system parameters, i.e., elastic modulus and modal damping coefficient, were investigated using seven CFRP specimens with different carbon fiber angles of 0°, 15°, 30°, 45°, 60°, 75°, and 90° [19]. The variations in both system parameters were measured using modular equipment and analyzed for two resonance frequencies.

Variations in the dynamic characteristics of CFRP specimens were studied for three factors, i.e., temperature, spectral loading pattern, and carbon fiber angle, to derive the modal parameters from the representative measured frequency response function (FRF). The relationship between the spectral loading pattern and carbon fiber angle [20] or the effect of temperature factor [21] was examined using a uniaxial excitation test. Variations in the FRF of CFRP specimens for the aforementioned three factors were simultaneously evaluated using the same uniaxial excitation [22]. The mode shapes of the CFRP specimens were compared using the modal assurance criterion, and the modal parameters were obtained via impact modal testing [23]. In that study [23], the boundary condition of the CFRP specimen was: clamped at one end of the rectangular specimen. In a recent study, impact modal testing was used to identify the CFRP specimens under free-free conditions, and a new mode-tracking method was proposed for a wide range of frequencies [24]. Particularly, the proposed mode tracking method was based on three indicators, i.e., resonance frequency, modal damping ratio, and modal assurance criterion (MAC), simultaneously, to obtain reliable mode tracking results for first five resonance frequencies. In this study, two sensitivity analysis formulations were proposed to identify the variation in the viscous damping coefficient with the increase in the carbon fiber angle: the direct partial derivatives of the viscous damping coefficient over the resonance frequency and modal damping ratio and the relative error of the viscous damping coefficient of carbon fiber. The relative error of the viscous damping coefficient of carbon fiber was formulated based on the assumption of the identified viscous damping coefficient, which is equivalent to the parallel relationship of the viscous damping coefficient between the binding matrix and carbon fiber. The direct derivatives of the equivalent viscous damping coefficient were not efficient in estimating the sensitivity of the CFRP structure over the carbon fiber angle because the considerable damping effect from the binding matrix does not change according to the carbon fiber angle. The modal parameters, i.e., the resonance frequency and modal damping ratio, were identified from the experimental modal analysis used for the sensitivity analysis of the viscous damping coefficient. Simple rectangular CFRP specimens (80 mm (W) × 150 mm (L) × 3 mm (H)) were prepared using 12 layers of unidirectional (UD) pre-implemented composites, and a modal test was conducted under free-free boundary conditions. The sensitivity analyses of the CFRP specimens were evaluated by comparing the first five mode shapes, i.e., three bending modes and two twisting modes. In reality, several factors are affected by the damping element of the CFRP structure, e.g., the inelastic behavior of carbon fiber and the interphase between the fiber and matrix, the slip at the fiber/matrix interface in the case of non-perfect adhesion, and the thermo-elastic behavior of the fiber and matrix, including the viscoelastic behavior of the composite structure [25]. The identified damping element of the CFRP structure was assumed to be dependent on the viscous damping behavior only. Therefore, the sensitivity results may be flawed if the effects of other damping factors are dominant compared with the viscous damping coefficient.

2. Sensitivity Formulation for the Viscous Damping Coefficient

The damping elements in mechanical systems can be categorized into three types: viscous damping, dry friction damping, and hysteretic damping. The dry friction damping

coefficient was constant in magnitude but opposite to the motion of the system. Hysteretic damping, the energy dissipation of which can be represented by the hysteresis loop in the stress–strain diagram, was caused by deformation of the material. Both aforementioned damping elements belong to the non-linear or non-energy conservative condition in mechanical systems, but viscous damping is a linear mechanical element, which is proportional to velocity.

The one degree-of-freedom (1-DOF) linear mechanical system can be expressed using three linear mechanical components, i.e., mass (m), spring coefficient (k) proportional to the displacement, and viscous damping coefficient (c), which is proportional to the velocity, as shown in Equation (1).

$$m\ddot{x}(t) + c\dot{x}(t) + kx(t) = F(t) \tag{1}$$

Here, $F(t)$, is the external force in a time domain, and $\ddot{x}(t)$ and $\dot{x}(t)$ are the second and first derivatives of displacement $x(t)$, respectively. The viscous damping coefficient in physical coordinates can be expressed using modal parameters, i.e., the resonance frequency $\omega_n = \sqrt{k/m}$ and modal damping ratio $\xi = c/(2m\omega_n)$. The transformed 1-DOF governing equations are shown in Equations (2) and (3) using modal parameters. The modal damping ratio ξ can be obtained using the relationship between the resonance frequency and the other two half-power frequencies [10,11].

$$\ddot{x} + 2\xi\omega_n\dot{x} + \omega_n^2 = f(t) \tag{2}$$

$$f(t) = \frac{F(t)}{m} \tag{3}$$

The 1-DOF system can be extended into an N-DOF system by applying a matrix formulation, as shown in Equation (4).

$$\begin{bmatrix} 1 & & zeros \\ & \ddots & \\ zeros & & 1 \end{bmatrix}\ddot{X} + \begin{bmatrix} 2\omega_{n,1}\xi_1 & & zeros \\ & \ddots & \\ zeros & & 2\omega_{n,N}\xi_N \end{bmatrix}\dot{X} + \begin{bmatrix} \omega_{n,1}^2 & & zeros \\ & \ddots & \\ zeros & & \omega_{n,N}^2 \end{bmatrix}X = \begin{bmatrix} f_1(t) \\ \vdots \\ f_N(t) \end{bmatrix} \tag{4}$$

Here, $X = \begin{bmatrix} x_1(t) & \ldots & x_N(t) \end{bmatrix}^T$ is a column vector in modal coordinates, and $\omega_{n,i}$, ξ_i, and F_i are the modal parameters of resonance frequency, modal damping coefficient, and mass-normalized external force, respectively, at the ith mode. CFRP is dependent on three factors: temperature (T), spectral loading pattern (p), and carbon fiber angle (θ). Therefore, the identified modal parameters were subjective for the three factors. The revised multi-DOF system for the CFRP structure is shown in Equation (5).

$$\begin{bmatrix} 1 & & zeros \\ & \ddots & \\ zeros & & 1 \end{bmatrix}\ddot{X} + \begin{bmatrix} 2\omega_{n,1}(T,\theta)\xi_1(T,p,\theta) & & zeros \\ & \ddots & \\ zeros & & 2\omega_{n,N}(T,\theta)\xi_N(T,p,\theta) \end{bmatrix}\dot{X}$$
$$+ \begin{bmatrix} (\omega_{n,1}(T,\theta))^2 & & zeros \\ & \ddots & \\ zeros & & (\omega_{n,N}(T,\theta))^2 \end{bmatrix}X = \begin{bmatrix} f_1(t) \\ \vdots \\ f_N(t) \end{bmatrix} \tag{5}$$

The main advantage of the multi-DOF system in modal coordinates is the decoupling of each mode by the representation of modal parameters. If both the parameters, i.e., temperature and spectral loading pattern, are not changed, the sensitivity of the viscous damping coefficient in the ith mode can be formulated with a small increase in modal parameters with an increase in the carbon fiber angle, as shown in Equation (6). It is assumed that the modal mass, m_i, does not change according to variation in the carbon

fiber angle. The viscous damping coefficient normalized by the modal mass is defined as the mass-normalized viscous damping coefficient in Equation (7).

$$\frac{\Delta c_i(\theta)}{\Delta\theta} = \frac{\Delta(2m_i\omega_{n,i}\xi_i)}{\Delta\theta} = 2m_i\left[\xi_i\frac{\Delta\omega_{n,i}}{\Delta\theta} + \omega_n\frac{\Delta\xi_i}{\Delta\theta}\right] \tag{6}$$

$$\overline{c}_i = \frac{c_i}{m_i} \tag{7}$$

CFRP consists of two main elements: a carbon fiber element and a binding matrix element. When the carbon fiber and binding matrix are merged into a single composite structure during the manufacturing processes—that is, hot-pressing—the viscous damping coefficient of the composite is not simply the summation of the viscous damping coefficients of each element. The viscous damping coefficient c_i is assumed to be a parallel combination of the carbon fiber and binding matrix if the CFRP structure can be allowed to be a linear system. As the carbon fiber angle increased, the viscous damping coefficient of the binding matrix did not change, but the viscous damping coefficient of the carbon fiber changed. The combination of the two materials can be assumed to be parallel in a linear system because CFRP is manufactured as a composite structure using carbon fiber and the binding matrix. If the ith mass-normalized viscous damping coefficient at the reference angle of the carbon fiber is defined as $\overline{c}_{def,i}$, the viscous damping coefficient is the equivalent viscous damping coefficient derived from two mass-normalized viscous damping coefficients, that is, the carbon fiber ($\overline{c}_{F,i}$) and binding matrix ($\overline{c}_{M,i}$), as shown in Equation (8). If the carbon fiber angle is increased by θ from the reference angle, the equivalent mass-normalized viscous damping coefficient ($\overline{c}_{eq,i}(\theta)$) can be expressed as a similar formulation using the constant mass-normalized damping coefficient of the binding matrix ($\overline{c}_{M,i}$) and mass-normalized damping coefficient of carbon fiber ($\overline{c}_{F,i}(\theta)$), as shown in Equation (9).

$$\frac{1}{\overline{c}_{def,i}} = \frac{1}{\overline{c}_{F0,i}} + \frac{1}{\overline{c}_{M0,i}} \tag{8}$$

$$\frac{1}{\overline{c}_{eq,i}(\theta)} = \frac{1}{\overline{c}_{F,i}(\theta)} + \frac{1}{\overline{c}_{M0,i}} \tag{9}$$

Equations (8) and (9) can be merged into one equation by eliminating the constant viscous damping coefficient, $\overline{c}_{M0,i}$, as shown in Equation (10).

$$\left(1 - \frac{\overline{c}_{F0,i}}{\overline{c}_{F,i}(\theta)}\right) = \overline{c}_{F0,i}\left(\frac{1}{\overline{c}_{def,i}} - \frac{1}{\overline{c}_{eq,i}(\theta)}\right) \tag{10}$$

The left term in Equation (10) is the formulation of the relative error between the viscous damping coefficients of carbon fiber, the increase in carbon fiber angle θ, and the reference angle. The right term is composed of two equivalent viscous damping coefficients, $\overline{c}_{def,i}$ and $\overline{c}_{eq,i}(\theta)$, which can be obtained from the experimental modal test. The sensitivity in Equation (6) is a general formulation that uses the derivative of the equivalent viscous damping coefficient of the CFRP structure; however, the direct derivatives of equivalent viscous damping may not represent the viscous damping coefficient because the damping coefficient of the binding matrix, $\overline{c}_{M0,i}$, does not change according to the carbon fiber angle. Therefore, the constant value of the damping coefficient of the binding matrix may distort the sensitivity result in Equation (6). As a result, the proposed sensitivity analysis of the viscous damping coefficient for only carbon fiber (Equation (10)) is more reasonable for identifying variations in the damping coefficient with the increase in the carbon fiber angle.

In practice, the sensitivity index for different carbon fiber angles in certain resonance modes is proposed under the discrete increase in the carbon fiber angle. The derivative of the mass-normalized viscous damping coefficient for the carbon fiber increase θ_k and the ith mode can be derived as the sensitivity index $I_{eq,i}(\theta_k)$ using the averaged modal damping ratio $\xi_{avg,\,k}$ and the averaged resonance frequency $\omega_{avg,\,k}$ in the $(k-1)$th angle and

kth angle ($k = 0$ is the default angle), as shown in Equation (11). The sensitivity index for a certain carbon fiber angle (θ_k) is formulated by dividing the 2-norm of all sets of sensitivity values. The sensitivity index of the carbon fiber only is also derived in a similar manner to Equation (11) by dividing the 2-norm of all sets of relative error values, as shown in Equation (12). $I_{F,i}(\theta_k)$ indicates the sensitivity of the carbon fiber to increase θ_k and the ith mode. The invariant variables, $2m_i$ in Equation (6) and $\bar{c}_{F0,i}$ in Equation (10), were eliminated for the final form in the sensitivity index.

$$I_{eq,i}(\theta_k) = \frac{\zeta_{avg,k}\frac{\Delta\omega_{n,i}}{\Delta\theta_k} + \omega_{avg,k}\frac{\Delta\zeta_i}{\Delta\theta_k}}{\text{norm}\left\{\sum_{k=1}^{N}\left[\zeta_{avg,k}\frac{\Delta\omega_{n,i}}{\Delta\theta_k} + \omega_{avg,k}\frac{\Delta\zeta_i}{\Delta\theta_k}\right]\right\}} \tag{11}$$

$$I_{F,i}(\theta_k) = \frac{\frac{1}{\bar{c}_{def,i}} - \frac{1}{\bar{c}_{eq,i}(\theta_k)}}{\text{norm}\left\{\sum_{k=1}^{N}\left[\frac{1}{\bar{c}_{def,i}} - \frac{1}{\bar{c}_{eq,i}(\theta_k)}\right]\right\}} \tag{12}$$

Here, N is the number of times the carbon fiber angle was increased, and θ_k is the increase in carbon fiber angle at the kth order.

3. Measurement of Modal Parameters

The modal parameters of CFRP were derived from a simple rectangular specimen (80 mm (W) × 150 mm (L) × 3 mm (H)). A large UD plate was prepared using 12 layers of pre-implemented composite fibers (USN 250A, SK Chemical, Seongnam, South Korea). The pre-implemented USN 250A comprised the UD carbon fibers (T700(12K), Toray, Tokyo, Japan) and the binding matrix, an epoxy resin. The large CFRP plate was manufactured via the hot-pressing process using 12 layers of USN 250A and cutting each specimen from the large CFRP plate at five different angles, 0°, 30°, 45°, 60°, and 90°. The configuration of the simple rectangular CFRP specimen and carbon fiber angle of the CFRP specimen are illustrated in Figures 1 and 2, respectively. The tested CFRP specimen, including the attached accelerometers, is shown in Figure 3.
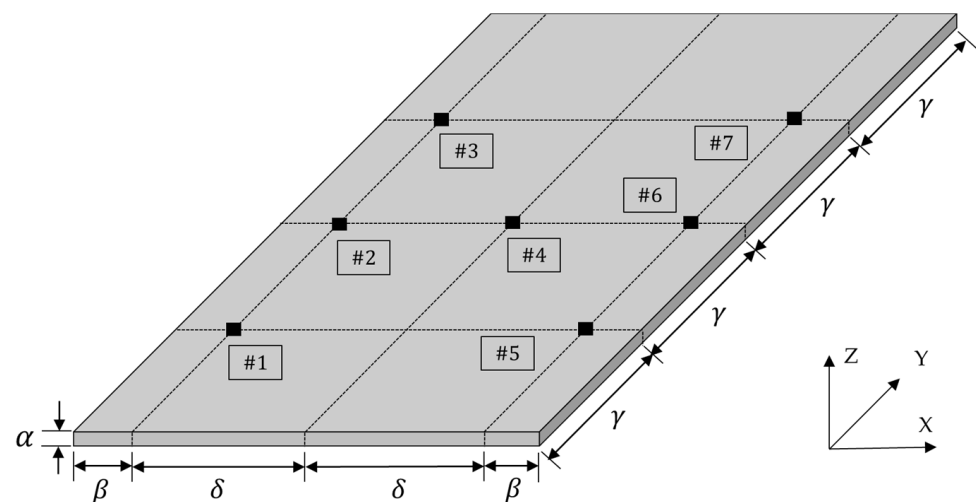

Figure 1. Configuration of a simple rectangular CFRP specimen with sensor locations (#1~#7); $\alpha = 3$ mm, $\beta = 10$ mm, $\gamma = 37.5$ mm, and $\delta = 30$ mm.
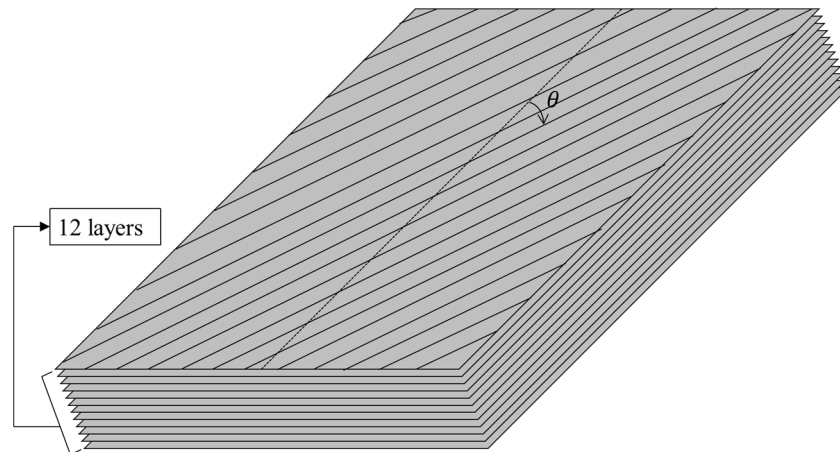
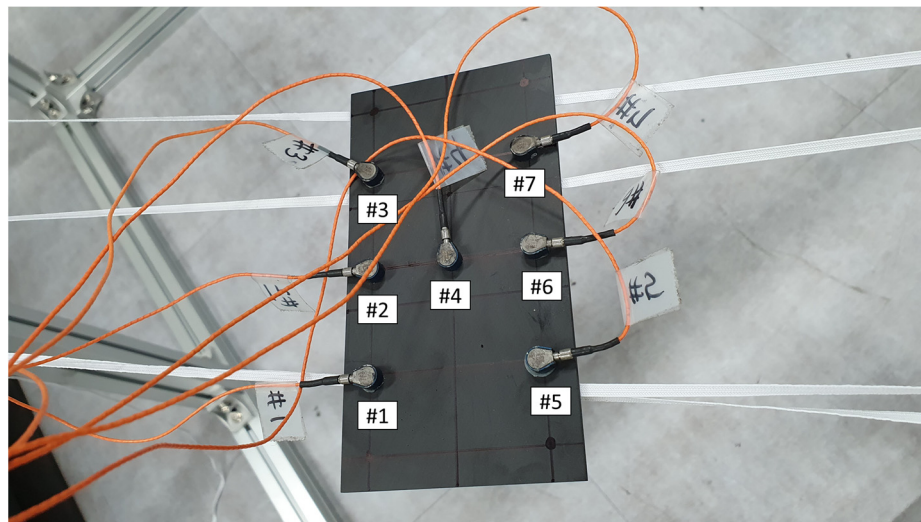**Figure 2.** Carbon fiber angle in the multi-layered CFRP specimen.

Figure 3. Configuration of 12 layers of UD pre-implemented composite fibers USN 250A.

Seven sensor locations (#1–#7) were selected to measure the response acceleration data in the CFRP specimen. The sensor locations are illustrated in Figure 1. All uniaxial accelerometers (model: 3225F2, Dytran, Chatsworth, CA, USA) were used for the vertical direction (z-axis only), and the verification of sensor location was previously performed by modal analysis of the finite element of the simple rectangular specimen model, as illustrated in Figure 4 [24]. The weight of the selected accelerometer was relatively small (1 g) compared with the weight of the CFRP specimen (56.5 g). Thus, the mass loading effect was minimized for the CFRP specimen. The beeswax manufactured by Dytran was used to prevent any addition of stiffness at the sensor attachment locations. The modal parameters were obtained via impact modal testing of the CFRP specimen under the impact force at #4 using an impact hammer (model: 5800B3, Dytran, Chatsworth, CA, USA). The measurement process for the experimental impact test was conducted using Test.Lab software (Siemens, Munich, Germany). FRFs were calculated using the average of 10 impact hammer tests at the same location, and fixed hammer conditions were used for the impact modal testing. The frequency band was set between 0.1 Hz and 4096 Hz, and the boundary condition of the simple CFRP specimen was set for free-free conditions by placing the specimen on the nest made using rubber bands with very low static stiffness, as shown in Figure 3. The experimental modal testing using an impact hammer was analyzed in the frequency domain so that the CFRP specimen suspended by the low static-stiffness rubber band did not distort the identified modal parameters

in a high-frequency range. Therefore, the boundary condition applied in Figure 3 can be assumed to be a free-free condition. Additionally, the reliability of the experimental modal test result was previously verified from the calculation of MAC between the experimental and theoretical eigenvectors from the finite model [24].
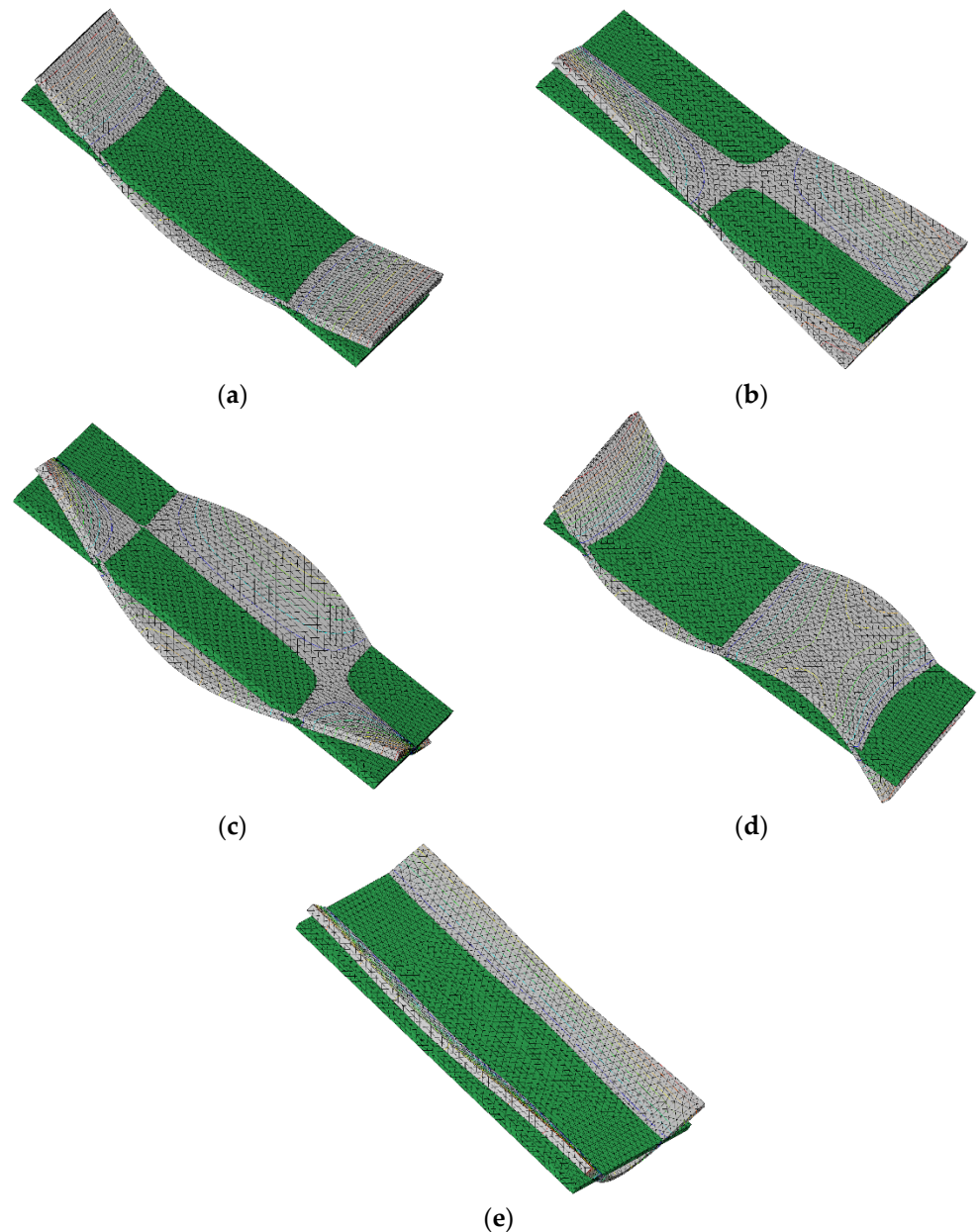

Figure 4. The mode shape of the FE model of simple specimens (grey color) overlapped with the original model (green color): (**a**) first mode (1st bending); (**b**) second mode (1st twisting); (**c**) third mode (2nd twisting); (**d**) fourth mode (2nd bending); and (**e**) fifth mode (3rd bending) [24].

The measured FRFs were used to identify the modal parameters, resonance frequency, and modal damping coefficient using the PolyMAX algorithm in Test.Lab software. The orthogonality of each mode was checked using the modal assurance criterion [10,11]. The identified modal parameters were the same as those in a previous study [24], as summarized in Table 1. The five mode shapes, i.e., three bending modes and two twisting modes, were tracked from the previous study by comparing them with the isotropic SS275 specimen.

Table 1. Measured modal parameters of the CFRP specimen for five different carbon fiber angles [24].

Specimen	Resonance Frequency (Hz)	Modal Damping Coefficient (%)	Mode Shape
$\theta_0 = 0°$	1149.1	0.4	Bending (first)
	1276.1	2.5	Twisting (first)
	1368.7	1.3	Twisting (second)
	2990.9	1.3	Bending (second)
	951.0	5.3	Bending (third)
$\theta_1 = 30°$	360.6	0.39	Bending (first)
	754.5	0.21	Twisting (first)
	941.1	0.82	Twisting (second)
	1657.6	0.01	Bending (second)
	1450.4	0.55	Bending (third)
$\theta_2 = 45°$	330.4	1.3	Bending (first)
	595.6	1.4	Twisting (first)
	878.0	1.0	Twisting (second)
	1568.9	1.2	Bending (second)
	1749.2	1.5	Bending (third)
$\theta_3 = 60°$	310.6	1.1	Bending (first)
	458.5	1.5	Twisting (first)
	979.0	1.3	Twisting (second)
	835.0	0.9	Bending (second)
	2690.4	3.9	Bending (third)
$\theta_4 = 90°$	305.1	0.9	Bending (first)
	380.0	1.7	Twisting (first)
	1938.5	3.7	Twisting (second)
	824.1	0.9	Bending (second)
	3305.1	5.3	Bending (third)

4. Sensitivity Analysis of the Viscous Damping Coefficient

Previous studies analyzed the modal damping coefficient of CFRP specimens according to the carbon fiber angle, but the modal damping coefficient cannot represent the variation of the viscous damping coefficient directly when the resonance frequencies also change, as shown in Equation (6). The mass-normalized viscous damping coefficients (Equation (7)) can be calculated from the resonance frequency and modal damping coefficient, and the results are illustrated in Figure 5.

The variation of the mass-normalized viscous damping coefficient ($\bar{c}_i$) in Figure 5 shows that the sensitivity of the modal coefficient ratio (ξ_i) reported in previous studies [24] did not coincide with the viscous damping coefficient, owing to the change in resonance frequency according to the carbon fiber angle. A direct comparison of the variation trend between the viscous damping coefficient and modal damping ratio was conducted by normalizing all magnitudes, as shown in Figure 6. The variation trend in the two normalized damping values was not matched for all angles of the carbon fiber. The error between the two damping values can be clearly seen in Figure 6.

Two different sensitivity analyses were conducted for two damping coefficients: the mass-normalized viscous damping coefficient (Equation (11)) and the viscous equivalent damping coefficient of the carbon fiber (Equation (12)), as illustrated in Figure 7. In each mode, the sensitivity value was calculated for four angles, $\theta_0 = 0°$ (default), $\theta_1 = 30°$, $\theta_2 = 45°$, $\theta_3 = 60°$, and $\theta_4 = 90°$. In the case of the mass-normalized viscous damping coefficient, the plus sign denotes an increase in the viscous damping coefficient with an increase in the carbon fiber angle, and the minus sign denotes the opposite result. In the case of the relative error of the viscous damping coefficient of carbon fiber, the plus sign denotes a large value of the viscous damping coefficient of the carbon fiber compared with that at the reference angle. The zero and minus signs for the viscous damping coefficient of

carbon fiber were assigned for equal and small values of the damping coefficient of carbon fiber, compared with that at the reference angle, respectively.
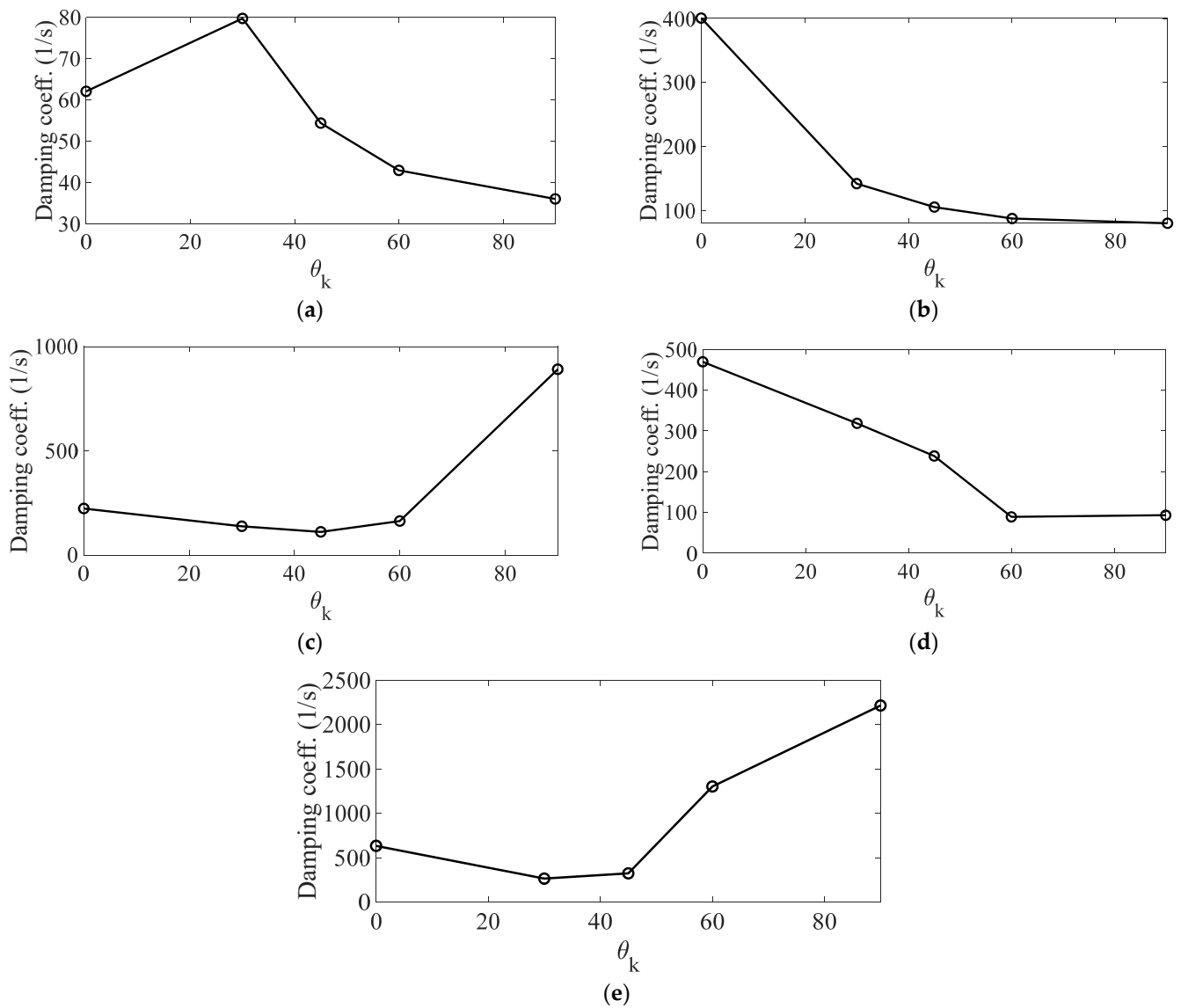

Figure 5. Variation of the mass-normalized viscous damping coefficient according to the carbon fiber angle: (**a**) First mode (1st bending); (**b**) Second mode; (1st twisting); (**c**) Third mode (2nd twisting); (**d**) Fourth mode (2nd bending); (**e**) Fifth mode (3rd bending).

The sensitivity analysis of the mass-normalized viscous damping coefficient shown in Figure 7 represents the variation in the viscous damping coefficient in Figure 5 according to the increase in the carbon fiber angle. However, the viscous damping coefficient was assumed to be the combined equivalent damping coefficient in the CFRP specimen, and the sensitivity result revealed little information regarding the specific variation of the carbon fiber or binding matrix in the composite structure, separately. The binding matrix condition was unchanged for all five CFRP specimens, and the carbon fiber angle was the only influential factor in the variation of the viscous damping coefficient of the CFRP specimens. Therefore, it was reasonable to assess the characteristics of the viscous damping of CFRP specimens using the sensitivity analysis of the viscous damping coefficient of carbon fiber only.
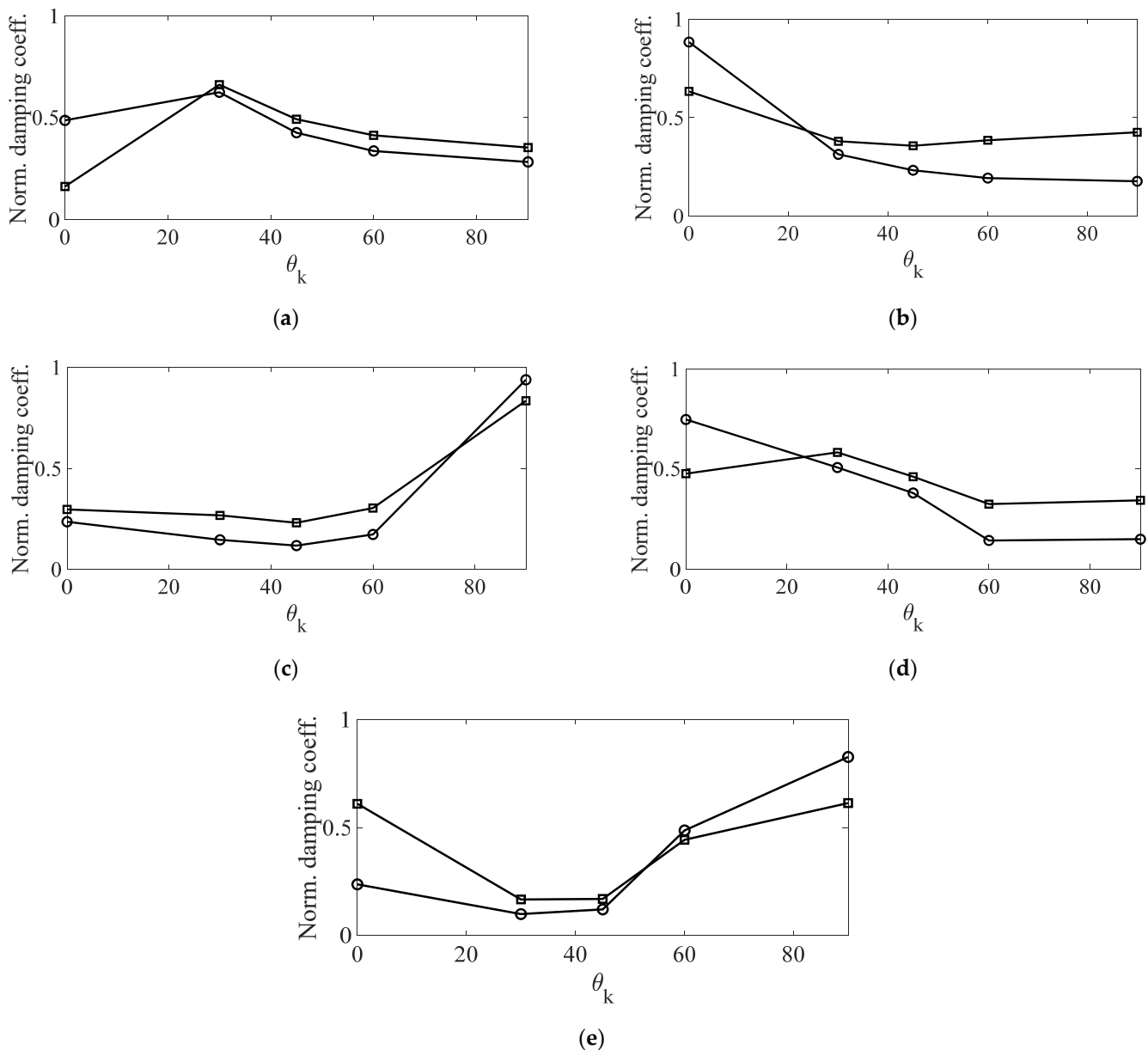
Figure 6. Comparison of normalized (magnitude) damping coefficient according to the carbon fiber angle, ⊖: viscous damping coefficient, ⊟: modal damping ratio, (**a**) First mode (1st bending) (**b**) Second mode (1st twisting) (**c**) Third mode (2nd twisting) (**d**) Fourth mode (2nd bending) (**e**) Fifth mode (3rd bending).

The sensitivity results from Figure 7 reveal that the sensitivity result from the first bending mode was approximately opposite to that from the third bending mode because the two bending mode shapes were orthogonal to each other (see Figure 4). Thus, the effect of the carbon fiber angle at θ_k for the first mode is similar to the effect of the carbon fiber angle at $90° - \theta_k$ for the third mode. The second bending mode case showed that sensitivity decreased with an increase in the carbon fiber angle. This seems to be a trend similar to that of the first bending case. In the first twisting mode case, the sensitivity value decreased with an increase in the carbon fiber angle, similar to the second bending mode case. In the second twisting mode case, the sensitivity decreased until $\theta_2 = 45°$ and then increased up to $\theta_4 = 90°$.
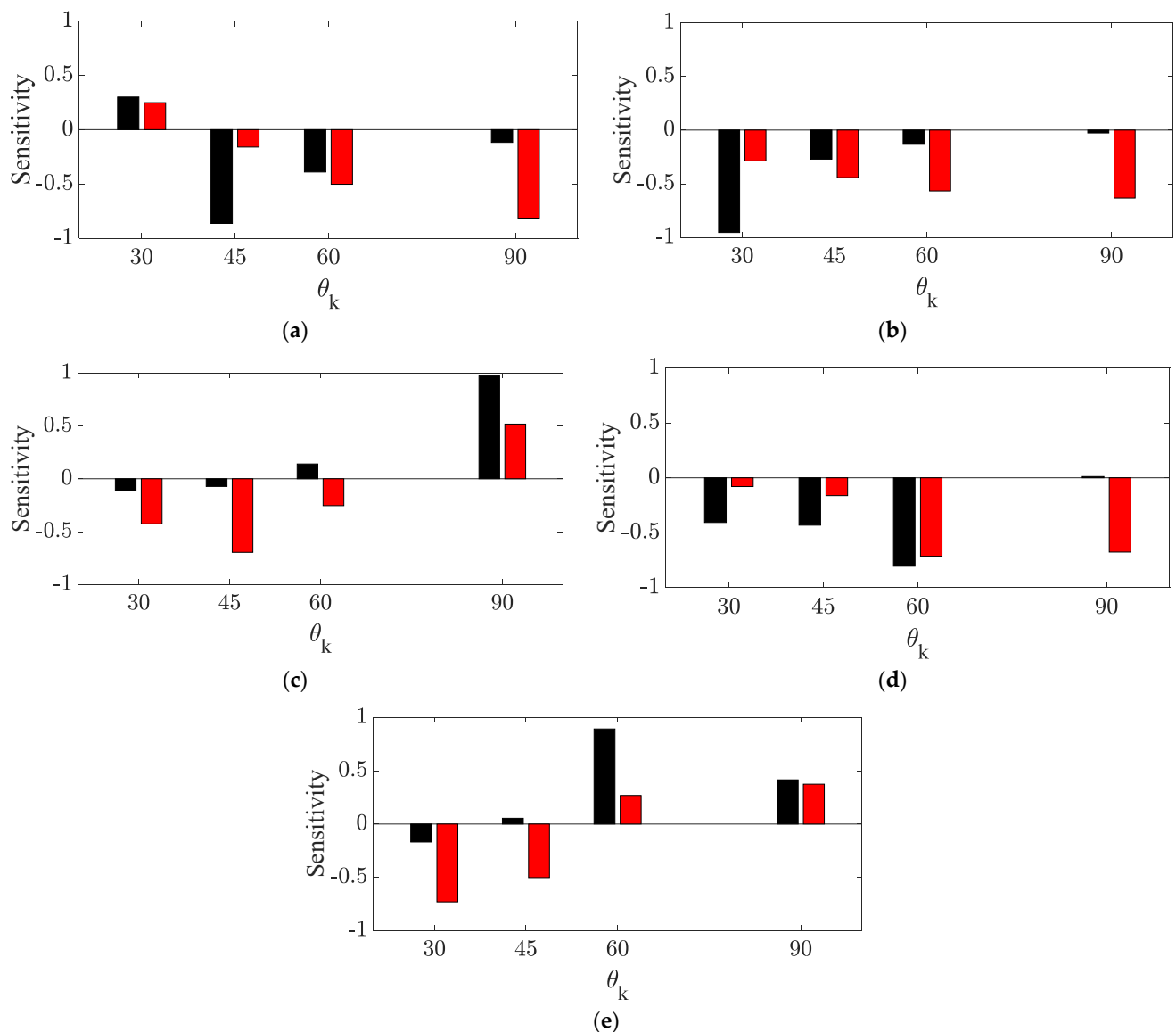
Figure 7. Sensitivity analysis results, ■: the mass-normalized equivalent viscous damping coefficient, ■: the viscous damping coefficient of the carbon fiber (**a**) First mode (1st bending) (**b**) Second mode (1st twisting) (**c**) Third mode (2nd twisting) (**d**) Fourth mode (2nd bending) (**e**) Fifth mode (3rd bending).

The sensitivity results for carbon fiber only matched well with the variation of resonance frequencies, as summarized in Table 1. The resonance frequencies decreased with an increase in the carbon fiber angle for the first bending mode, second bending mode, and first twisting mode. The resonance frequency increased with an increase in the carbon fiber angle for the third bending mode. For the second bending mode, the minimum resonance frequency was at $\theta_2 = 45°$, and this value increased when the carbon fiber angle was increased or decreased. Therefore, it can be concluded that the viscous damping coefficient of carbon fiber is proportional to the structural stiffness (or elastic modulus [25]), which is directly related to the resonance frequency. In particular, the viscous damping coefficient of carbon fiber may considerably influence the equivalent viscous damping coefficient of the CFRP structure, even at a relatively small value compared with that of the binding matrix, because two viscous damping coefficients, the carbon fiber and the binding matrix, were combined as a parallel combination. Therefore, sensitivity analysis of the viscous damping coefficient of carbon fiber in Equation (11) should be conducted to understand the viscous damping element of the CFRP structure for different carbon fiber angles. Here, the sensitiv-

ity results may change even for the same CFRP specimen when the boundary conditions change from the current free-free condition to other clamped conditions. The proposed sensitivity index is dependent on the modal parameters, so the derived results in Figure 7 will change according to variations in the dynamic characteristics of the CFRP specimen.

5. Conclusions

Focusing on the sensitivity of the viscous damping coefficient of CFRP specimens, two sensitivity analysis formulations were proposed to understand the variation in the viscous damping coefficient over the carbon fiber angle. The modal parameters identified from the experimental impact test were taken from a previous study [24], and sensitivity analysis was performed using the viscous damping coefficient instead of the modal damping ratio. Both damping coefficients, the mass-normalized viscous damping coefficient and the modal damping ratio, were compared, and errors were found between them, owing to variation in resonance frequencies. The sensitivity analysis from the direct derivative of the viscous damping coefficient could not adequately explain the variation in the parallel combination of the viscous damping coefficient between the carbon fiber and the binding matrix. A new sensitivity analysis formulation was proposed as the formulation of the relative error of the viscous damping coefficient between the increased carbon fiber angle and the reference one because variation in the viscous damping coefficient was only dependent on the viscous damping coefficient of carbon fiber. From the proposed sensitivity analysis of carbon fiber, it can be seen that the viscous damping coefficient of carbon fiber is proportional to the structural stiffness, which is directly related to the resonance frequency. The sensitivity of the viscous damping coefficient of carbon fiber was considerable for the equivalent viscous damping coefficient of the CFRP structure under the parallel combination of viscous damping coefficients between the carbon fiber and the binding matrix. As a result, the proposed sensitivity index of carbon fiber only is the effect criterion for evaluating the damping behavior of the CFRP structure for different carbon fiber angles.

Data Availability Statement: The data presented in this study are available on request from the corresponding author.

Conflicts of Interest: The authors declare no conflict of interest.

Nomenclature

m	mass of a 1-DOF (degree of freedom) system
m_i	modal mass at ith mode of multi-DOF system
k	stiffness coefficient of a 1-DOF system
$F(t)$	external force at a 1-DOF system
$f(t)$	mass-normalized external force at a 1-DOF system
$f_i(t)$	ith mass-normalized external force at multi-DOF system
ξ	viscous damping ratio of a 1-DOF system
ξ_i	ith viscous damping ratio at multi-DOF system
c	damping coefficient of 1-DOF system
c_i	viscous damping coefficient at ith mode
$\bar{c}_i$	mass normalized viscous damping coefficient at ith mode
N	Maximum number of DOF at multi-DOF system
T	temperature variable
p	spectral loading pattern variable
θ	carbon fiber angle variable
θ_k	kth carbon fiber angle variable of carbon-fiber-reinforced plastic specimen
Δ	derivative variable

$\bar{c}_{def,i}$	mass-normalized equivalent viscous damping coefficient at ith mode
$\bar{c}_{eq,i}(\theta_k)$	mass-normalized equivalent viscous damping coefficient at ith mode, the carbon fiber angle θ_k
$\bar{c}_{M0,i}$	mass-normalized viscous damping coefficient of binding matrix
$\bar{c}_{F0,i}$	mass-normalized viscous damping coefficient of carbon fiber at default carbon fiber angle ($\theta_1 = 0^o$)
$\bar{c}_{F,i}(\theta_k)$	mass-normalized viscous damping coefficient of carbon fiber at carbon fiber angle θ_k
$\xi_{avg,k}$	averaged modal damping ratio in the $(k{-}1)$th carbon angle and kth carbon angle
$\omega_{avg,k}$	averaged resonance frequency in the $(k{-}1)$th carbon angle and kth carbon angle
$I_{eq,i}(\theta_k)$	sensitivity index based on the partial derivatives of $\bar{c}_{eq,i}(\theta_k)$ with respect to the resonance frequency and modal damping ratio at ith mode, the carbon fiber angle θ_k
$I_{F,i}(\theta_k)$	sensitivity index based on the viscous damping coefficient of carbon fiber at ith mode, the carbon fiber angle θ_k

References

1. Lamberti, A.; Chiesura, G.; Luyckx, G.; Degrieck, J.; Kaufmann, M.; Vanlanduit, S. Dynamic Strain Measurements on Automotive and Aeronautic Composite Components by Means of Embedded Fiber Bragg Grating Sensors. *Sensors* **2015**, *15*, 27174–27200. [CrossRef]
2. Aggogeri, F.; Borboni, A.; Merlo, A.; Pellegrini, N.; Ricatto, R. Vibration Damping Analysis of Lightweight Structures in Machine Tools. *Materials* **2017**, *10*, 297. [CrossRef]
3. Xu, W.; Cao, M.; Ding, K.; Radzieński, M.; Ostachowicz, W. Crack Identification in CFRP Laminated Beams Using Multi-Resolution Modal Teager–Kaiser Energy under Noisy Environments. *Materials* **2017**, *10*, 656. [CrossRef]
4. Mencattelli, L.; Pinho, S.T. Realising bio-inspired impact damage-tolerant thin-ply CFRP Bouligand structures via promoting diffused sub-critical helicoidal damage. *Compos. Sci. Technol.* **2019**, *182*, 107684. [CrossRef]
5. Shevtsov, S.; Chebanenko, V.; Shevtsova, M.; Chang, S.-H.; Kirillova, E.; Rozhkov, E. On the Directivity of Lamb Waves Generated by Wedge PZT Actuator in Thin CFRP Panel. *Materials* **2020**, *13*, 907. [CrossRef] [PubMed]
6. Xu, J.; Deng, Y.; Wang, C.; Liang, G. Numerical model of unidirectional CFRP in machining: Development of an amended friction model. *Compos. Struct.* **2021**, *256*, 113075. [CrossRef]
7. Nikhamkin, M.S.; Semenov, S.V.; Solomonov, D.G. Application of experimental modal analysis for identification of laminated carbon fiber-reinforced plastic model parameters. In *ICIE2018, Proceedings of the 4th International Conference on Industrial Engineering, Lecture Notes in Mechanical Engineering, Moscow, Russia, 15–18 May 2018*; Radionov, A.A., Kravchenko, O.A., Guzeev, V.I., Rozhdestvenskiy, Y.V., Eds.; Springer: Cham, Switzerland; pp. 487–497. [CrossRef]
8. Garcia, C.; Trendafilova, I.; Zucchelli, A. The Effect of Polycaprolactone Nanofibers on the Dynamic and Impact Behavior of Glass Fibre Reinforced Polymer Composites. *J. Compos. Sci.* **2018**, *2*, 43. [CrossRef]
9. Khalid, M.; Rashid, A.; Arif, Z.; Akram, N.; Arshad, H.; Márquez, F.G. Characterization of Failure Strain In Fiber Reinforced Composites: Under On-Axis and Off-Axis Loading. *Crystals* **2021**, *11*, 216. [CrossRef]
10. Ewins, D.J. *Modal Testing*, 2nd ed.; Research Studies Press Ltd.: Hertfordshire, UK, 2000.
11. Inman, D.J. *Engineering Vibration*, 4th ed.; Pearson: Singapore, 2013.
12. Surgeon, M.; Wevers, M. Modal analysis of acoustic emission signals from CFRP laminates. *NDT E Int.* **1999**, *32*, 311–322. [CrossRef]
13. Ding, G.; Xie, C.; Zhang, J.; Zhang, G.; Song, C.; Zhou, Z. Modal analysis based on finite element method and experimental validation on carbon fibre composite drive shaft considering steel joints. *Mater. Res. Innov.* **2015**, *19*, S5-748–S5-753. [CrossRef]
14. Jinguang, Z.; Hairu, Y.; Guozhi, C.; Zeng, Z. Structure and modal analysis of carbon fiber reinforced polymer raft frame. *J. Low Freq. Noise Vib. Act. Control.* **2018**, *37*, 577–589. [CrossRef]
15. Troncossi, M.; Taddia, S.; Rivola, A.; Martini, A. Experimental Characterization of a High-Damping Viscoelastic Material Enclosed in Carbon Fiber Reinforced Polymer Components. *Appl. Sci.* **2020**, *10*, 6193. [CrossRef]
16. Cosco, F.; Serratore, G.; Gagliardi, F.; Filice, L.; Mundo, D. Experimental Characterization of the Torsional Damping in CFRP Disks by Impact Hammer Modal Testing. *Polymers* **2020**, *12*, 493. [CrossRef] [PubMed]
17. Schultz, A.B.; Tsai, S.W. Dynamic Moduli and Damping Ratios in Fiber-Reinforced Composites. *J. Compos. Mater.* **1968**, *2*, 368–379. [CrossRef]
18. Kozlowska, J.; Boczkowska, A.; Czulak, A.; Przybyszewski, B.; Holeczek, K.; Stanik, R.; Gude, M. Novel MRE/CFRP sandwich structures for adaptive vibration control. *Smart Mater. Struct.* **2016**, *25*, 35025. [CrossRef]
19. Dannemann, M.; Holeczek, K.; Leimert, J.; Friebe, S.; Modler, N. Adapted measuring sequence for the determination of directional-dependent dynamic material properties using a bending resonance method. *Polym. Test.* **2019**, *79*, 106044. [CrossRef]
20. Kim, C.-J. Sensitivity Analysis of the Frequency Response Function of Carbon-Fiber-Reinforced Plastic Specimens for Different Direction of Carbon Fiber as Well as Spectral Loading Pattern. *Materials* **2019**, *12*, 2983. [CrossRef]
21. Kang, H.-Y.; Kim, C.-J.; Lee, J. Modal Damping Coefficient Estimation of Carbon-Fiber-Reinforced Plastic Material Considering Temperature Condition. *Materials* **2020**, *13*, 2872. [CrossRef]

22. Kim, C.-J. Temperature-Dependent Dynamic Characteristics of Carbon-Fiber-Reinforced Plastic for Different Spectral Loading Patterns. *Materials* **2020**, *13*, 5238. [CrossRef]
23. Kim, C.-J. Comparison of Mode Shapes of Carbon-Fiber-Reinforced Plastic Material Considering Carbon Fiber Direction. *Crystals* **2021**, *11*, 311. [CrossRef]
24. Kim, C.J. Mode order tracking of carbon-fiber-reinforced plastic structure using multiple indicators. *Appl. Sci.* **2021**. submitted for publication.
25. Sol, H.; Rahier, H.; Gu, J. Prediction and Measurement of the Damping Ratios of Laminated Polymer Composite Plates. *Materials* **2020**, *13*, 3370. [CrossRef] [PubMed]